Original Article

Construction of a prognostic signature for breast cancer based on genes involved in unsaturated fatty acid biosynthesis

Hua Meng[1], Shuangyi Zhang[2], Min Ling[2], Yuanyuan Hu[1], Xiaohong Xie[1]

[1]Department of Breast Surgery, The First Affiliated Hospital of Zhejiang Chinese Medical University (Zhejiang Provincial Hospital of Chinese Medicine), Hangzhou, China; [2]The First Clinical College, Zhejiang Chinese Medical University, Hangzhou, China

Contributions: (I) Conception and design: H Meng, S Zhang, M Ling; (II) Administrative support: Y Hu, X Xie; (III) Provision of study materials or patients: Y Hu, X Xie; (IV) Collection and assembly of data: H Meng, S Zhang, M Ling; (V) Data analysis and interpretation: H Meng, S Zhang, M Ling; (VI) Manuscript writing: All authors; (VII) Final approval of manuscript: All authors.

Correspondence to: Yuanyuan Hu, MD; Xiaohong Xie, MD. Department of Breast Surgery, The First Affiliated Hospital of Zhejiang Chinese Medical University (Zhejiang Provincial Hospital of Chinese Medicine), No. 54, Youdian Road, Shangcheng District, Hangzhou 310001, China. Email: hyy_1214@163.com; xxh20230131@163.com.

Background: The biosynthesis of unsaturated fatty acids (UFAs) has been implicated in the onset and advancement of breast cancer (BC). This study aimed to develop molecular subtypes and prognostic signatures for BC based on UFA-related genes (UFAGs).

Methods: This study integrates multi-omics and survival data from public databases to elucidate molecular classifications and risk profiles based on UFAGs. Consensus clustering and Lasso Cox regression methodologies are employed for subtype identification and risk signature development, respectively. Immune microenvironment assessment is conducted using CIBERSORT and ESTIMATE algorithms, while drug sensitivity and response to immunotherapy are evaluated via pRRophetic and TIDE methods. Gene set enrichment analysis augments signature characterization, followed by nomogram construction and validation.

Results: We successfully identified two distinct BC molecular subtypes with significantly different prognoses utilizing UFAGs correlated with outcomes. A prognostic signature comprising three UFAGs [acetyl-CoA acyltransferase 1 (*ACAA1*), acyl-CoA thioesterase 2 (*ACOT2*), and ELOVL fatty acid elongase 2 (*ELOVL2*)] is developed, stratifying patients into high- and low-risk groups exhibiting divergent outcomes, clinicopathological traits, gene expression patterns, immune infiltration profiles, therapeutic susceptibility, and immunotherapy responses. The signature demonstrates robust prognostic performance in both training and validation cohorts, emerging as an independent predictor alongside age, which is integrated into a nomogram. Decision curve analysis highlights the nomogram's superiority over other factors in prognosis prediction. Calibration plots and receiver operating characteristic curves affirm its excellent performance in BC prognosis assessment.

Conclusions: Expression profiles of UFAGs are associated with BC prognosis, enabling the creation of a risk signature with implications for understanding the molecular mechanisms underlying BC progression.

Keywords: Unsaturated fatty acids (UFAs); breast cancer (BC); consensus clustering; immune microenvironment; nomogram

Submitted Sep 10, 2024. Accepted for publication Dec 17, 2024. Published online Feb 24, 2025.
doi: 10.21037/tcr-24-1668
View this article at: https://dx.doi.org/10.21037/tcr-24-1668

Introduction

Breast cancer (BC) stands as a global health crisis, accounting for 11.7% of all new cancer diagnoses in women, totaling approximately 2.3 million cases annually, outnumbering lung cancer as the most prevalent form of malignancy (1). This disease is characterized by a complex interplay of metastatic heterogeneity and biological plasticity, enabling it to variably colonize vital organs including the brain, lungs, liver, and bones (2). Despite significant progress in therapeutic strategies, the invasive nature of BC continues to pose challenges, resulting in less than desirable prognoses (3). A central challenge in BC management stems from its profound heterogeneity, manifesting not only biologically but also in patient outcomes. Initial strides in personalized medicine through estrogen receptor (ER) and human epidermal growth factor 2 (HER2) tumor stratification paved the way for targeted therapies (4). However, the quest for precision has since evolved towards molecular subtyping, epitomized by the groundbreaking Prediction Analysis of Microarray 50 (PAM50) classifier. This system, rooted in RNA expression patterns, categorizes tumors into five intrinsic subtypes: basal, HER2-enriched, Luminal A, Luminal B, and normal-like, enhancing our ability to tailor treatments accordingly (5). Despite these advancements, the clinical landscape remains fraught with variability in patient responses, even among those sharing similar molecular subtypes and clinical profiles. Early diagnosis vastly improves outcomes, with stage I BC patients experiencing a nearly 100% 5-year survival rate compared to just 26% for those diagnosed at stage IV (6).

Highlight box

Key findings

- A risk signature composed of unsaturated fatty acids (UFAs)-related genes can indicate prognosis and treatment response in breast cancer (BC) patients.

What is known and what is new?

- Reliable prognostic signatures are needed for evaluating BC outcomes. UFAs are closely associated with cancer, and their related genes can be used to predict tumor prognosis.
- This study developed a prognostic model for BC using three UFAs-related genes, which demonstrates predictive capabilities for overall survival, chemotherapy sensitivity, and immunotherapy responses.

What is the implication, and what should change now?

- This research provided UFAs-related biomarkers that can be used for prognostic or predictive purposes.

Yet, the presence of undetected advanced-stage or metastatic disease at initial diagnosis persists as a formidable obstacle. Thus, the pursuit of novel biomarkers and therapeutic modalities is imperative to further refine prognosis and treatment efficacy.

Lipid metabolism is integral to the onset and progression of neoplastic transformations, with dysregulated lipid metabolic pathways being a hallmark of malignant cells (7). This notion is fortified by observations of altered lipid profiles in various tumors, including BC (8), lung cancer (9), renal carcinoma (10), and hepatocellular carcinoma (11). Likewise, BC cells exhibit dysregulated expression of genes encoding enzymes involved in lipid biosynthesis (12), further emphasizing the significance of lipid metabolism perturbations in oncogenesis. In concordance with its pivotal role in tumor initiation and progression, fatty acids, as paramount products of lipid synthesis, have been implicated in cellular survival, malignancy, metastasis, and immune phenotypes across different cancers (13). Furthermore, supplemental intake of unsaturated fatty acids (UFAs) has demonstrated substantial benefits in cardiovascular diseases (14), inflammatory conditions (15), and nutritionally linked malignancies such as colorectal cancer (16), whereas excessive saturated fatty acid consumption is a recognized risk factor for the latter (17). Notably, UFAs supplementation has been shown to enhance chemosensitivity in multidrug-resistant cancer cells (18,19), albeit the precise mechanisms governing their role in BC progression remain elusive.

This study aimed to conduct a comprehensive bioinformatics analysis of The Cancer Genome Atlas (TCGA) dataset, integrating gene expression profiling, immune infiltration assessment, and clinical data examination, to investigate and validate the potential of unsaturated fatty acid-related genes (UFAGs) as novel prognostic biomarkers in BC patients. Furthermore, the establishment of a new three-gene risk score signature and nomogram derived from this analysis is anticipated to facilitate the surveillance and prediction of survival outcomes in BC patients, thereby enhancing personalized therapeutic strategies and patient management. We present this article in accordance with the TRIPOD reporting checklist (available at https://tcr.amegroups.com/article/view/10.21037/tcr-24-1668/rc).

Methods

Data acquisition and processing

Transcriptomic and clinical-pathological data for the TCGA-breast invasive carcinoma (BRCA) cohort were

retrieved from TCGA (https://portal.gdc.cancer.gov/). Following exclusion of cases with follow-up less than 30 days or incomplete clinical information, a total of 1,095 BC patients were included. Their transcriptomic data, transformed to log [fragments per kilobase of transcript per million mapped reads (FPKM) + 1], was utilized for prognostic analyses and model development. Additionally, the Vijver2002 cohort, consisting of 295 BC cases with transcriptomic and survival data, was obtained from the University of California Santa Cruz (UCSC, https://genome.ucsc.edu) database for model validation. Additionally, we downloaded the BC immunotherapy cohort GSE173839 from the Gene Expression Omnibus (GEO) database (https://www.ncbi.nlm.nih.gov/geo/) to evaluate the response to immunotherapy. A list of 28 UFAGs was compiled from the Kyoto Encyclopedia of Genes and Genomes (KEGG, https://www.kegg.jp/), detailed in Table S1. The study was conducted in accordance with the Declaration of Helsinki (as revised in 2013).

Consensus clustering analysis

Significantly survival-associated UFAGs were initially identified through univariate Cox regression ($P<0.05$), guiding molecular clustering. ConsensusClusterPlus package (20) was employed with settings for k=6 clusters, 50 resamplings, partitioning around medoids algorithm, and Pearson correlation distance. Kaplan-Meier (KM) survival analysis with log-rank tests assessed cluster differences, complemented by principal component analysis (PCA) of survival-associated UFAGs.

Risk signature construction and evaluation

Post intersection of survival-associated UFAGs with the Vijver2002 dataset, Lasso Cox regression implemented in glmnet with 1,000 times k-fold cross-validation was performed. Genes with non-zero coefficients were selected for the risk model formulation: riskscore = $\sum(\beta i \times Expr\_i)$, where βi denotes the coefficient of gene i and Expr_i its expression level. Patients were stratified into high- and low-risk groups based on the median riskscore, followed by KM survival analysis and PCA. Receiver operating characteristic (ROC) curves assessed the predictive power of the riskscore.

Gene set enrichment analysis

Differential expression analysis was conducted using the limma package, and genes with $|\log_2 (\text{fold change})| > 1$ were considered as differentially expressed. Gene set enrichment analysis based on Gene Ontology (GO) and KEGG pathways was performed using the clusterProfiler package (21) to determine the latent discrepancies in the biological function and signaling pathways between the high- and low-risk groups, at a significance threshold of $P<0.05$.

Immune infiltration assessment

Cibersort, integrated in Immuno-Oncology Biological Research (IOBR) package (22), estimated immune cell infiltration. Expression-based Estimation of Stromal and Immune Cells in Tumoral Tissue Environment (ESTIMATE) scores for immune and stromal components were also calculated within this package, with inter-group comparisons made using Wilcoxon tests.

Somatic mutation analysis

Somatic mutation data from the TCGA-BRCA cohort was analyzed and visualized through maftools.

Drug sensitivity and immunotherapy response assessment

Drug sensitivity was predicted using pRRophetic package (23), comparing the response of 45 drugs between high- and low-risk groups. Tumor Immune Dysfunction and Exclusion (TIDE) scores were calculated to evaluate immune therapy responsiveness, examining differences, correlations with riskscore, and responder variations between risk groups. Additionally, we evaluated the performance of UFAGs and the riskscore in predicting the outcome of immunotherapy in the GSE173839 cohort using binary logistic regression and ROC curve analysis, calculating the area under the curve (AUC). We used Wilcoxon tests to assess the differences in risk scores between complete responders (CRs) and non-responders (NRs).

Nomogram construction and evaluation

Prognostic factors for BC were screened by univariate and multivariate Cox regression ($P<0.05$), informing nomogram construction using rms. Calibration plots and ROC curves validated the nomogram's performance. Decision curve analysis with rmda package appraised the nomogram's superiority over other prognostic indicators in BC prognosis.

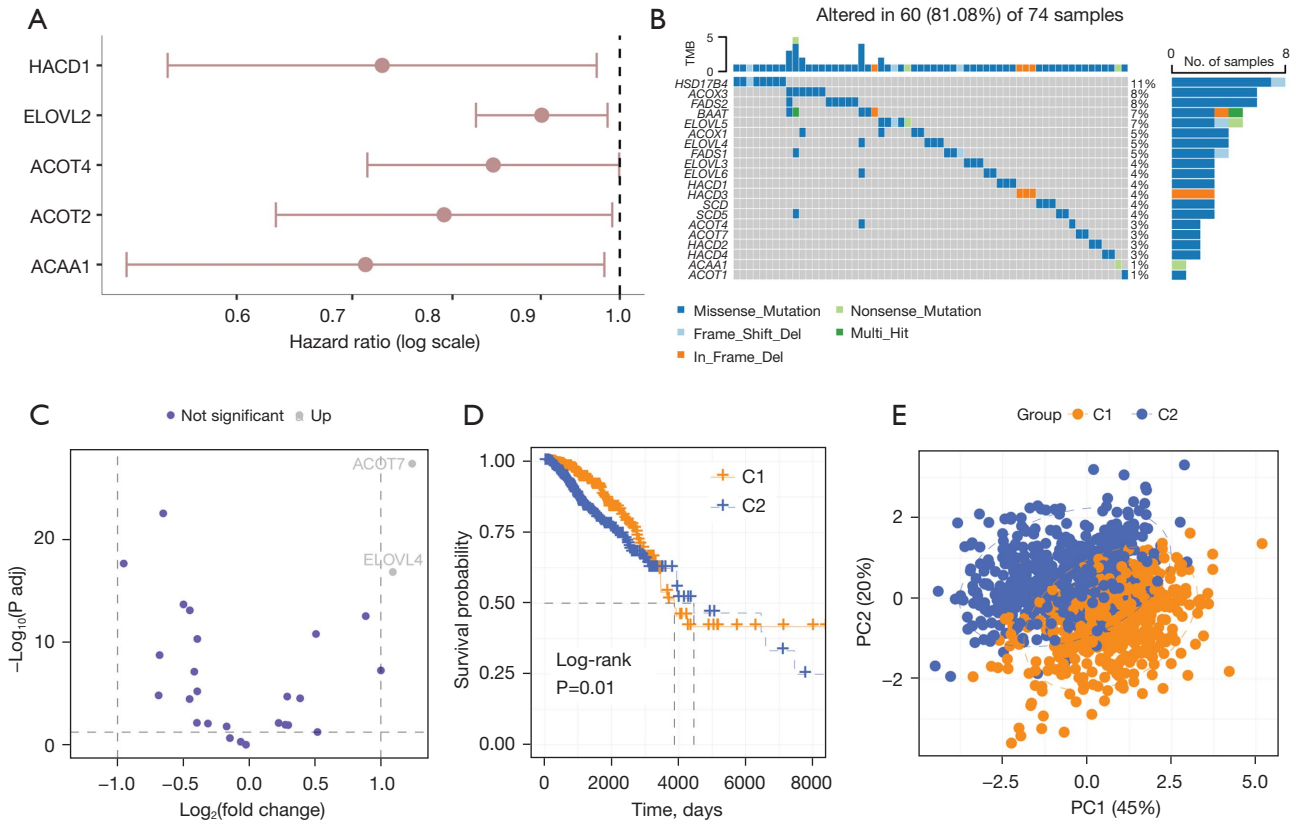

Figure 1 Expression, prognostic, and mutational characteristics of unsaturated fatty acid-associated genes in the TCGA-BRCA cohort. (A) Identification of five UFAGs significantly associated with breast cancer prognosis through univariate Cox regression analysis. (B) Oncoplot illustrating somatic mutations of UFAGs in the TCGA-BRCA cohort. (C) Volcano plot depicting differential expression analysis of UFAGs in the TCGA-BRCA cohort. (D) Kaplan-Meier survival curves distinguishing two subtypes derived from consensus clustering. (E) Principal component analysis effectively separating C1 and C2 subtypes based on five prognostic UFAGs in the TCGA-BRCA cohort. TCGA, The Cancer Genome Atlas; BRCA, breast invasive carcinoma; UFAG, unsaturated fatty acids-related genes; HACD1, 3-hydroxyacyl-CoA dehydratase 1; ELOVL2, ELOVL fatty acid elongase 2; ACOT4, acyl-CoA thioesterase 4; ACOT2, acyl-CoA thioesterase 2; ACOT1, acyl-CoA thioesterase 1; PC, principal component; TMB, tumor mutation burden.

Statistical analysis

Data analysis and visualization were conducted using R software (version 4.4.1). Prognostic differences were evaluated using KM survival curves and compared with the log-rank test. Between-group differences were assessed using Wilcoxon rank-sum tests, while Pearson correlation analysis was employed to evaluate the strength and direction of linear relationships between variables.

Results

Expression and prognostic significance of UFAGs

Univariate Cox regression analysis revealed that 5 out of 28 UFAGs were significantly associated with BC prognosis, including acyl-CoA thioesterase 4 (*ACOT4*), *ACOT2*, acetyl-CoA acyltransferase 1 (*ACAA1*), 3-hydroxyacyl-CoA dehydratase 1 (*HACD1*), and ELOVL fatty acid elongase 2 (*ELOVL2*) (*Figure 1A*). Somatic mutation analysis indicated a low mutation frequency among UFAGs in BC, primarily consisting of missense mutations, with hydroxysteroid 17-beta dehydrogenase 4 (*HSD17B4*) exhibiting the highest mutation rate (*Figure 1B*). Differential expression analysis pinpointed *ACOT7* and *ELOVL4* as significantly upregulated in BC (*Figure 1C*). Consensus clustering based on these 5 prognostically relevant UFAGs delineated two subtypes (C1 and C2), with significant survival disparity (*Figure 1D*). PCA further emphasized clear segregation

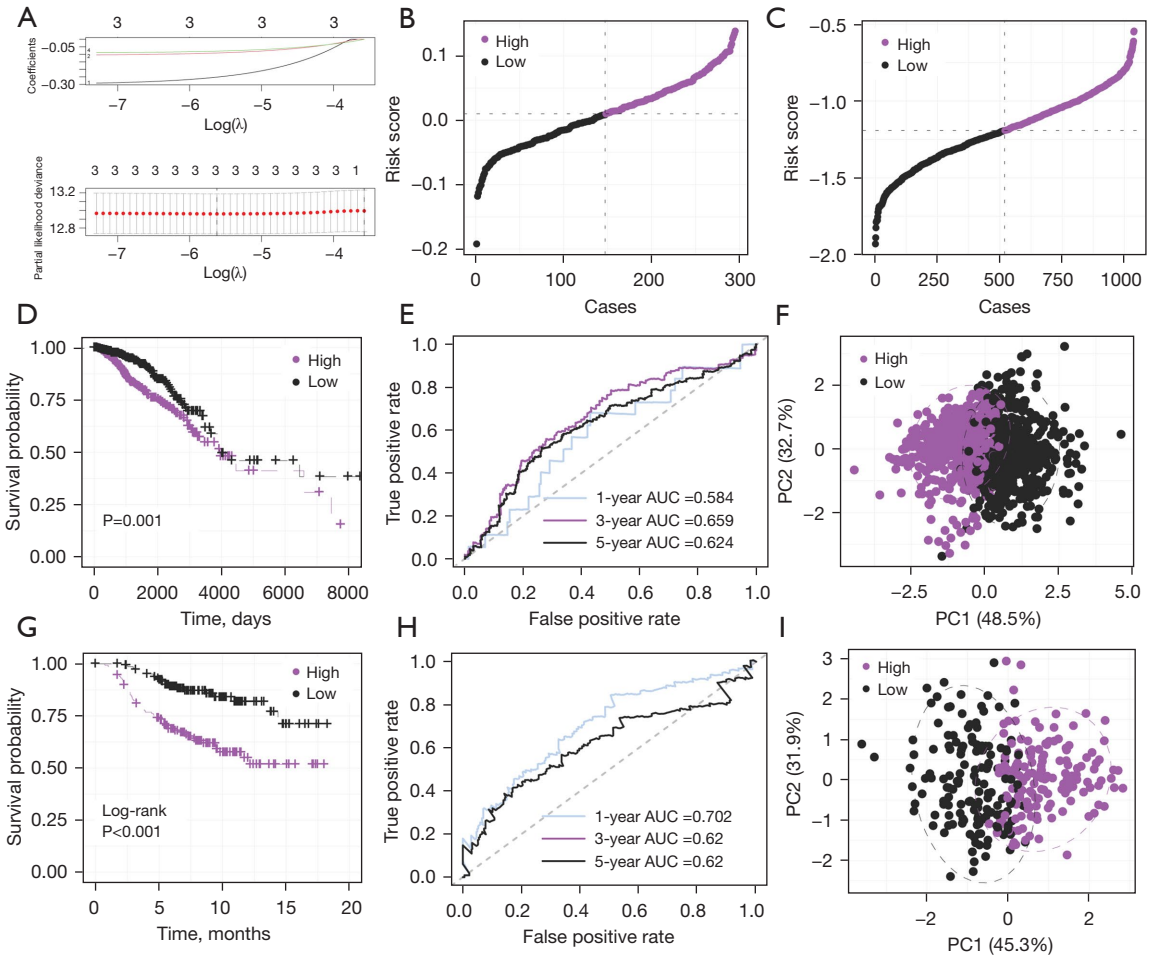

Figure 2 Construction and evaluation of UFAGs-related risk signature. (A) Lasso Cox regression analysis for feature selection. (B,C) Risk score distribution and patient stratification in the TCGA-BRCA and Vijver2002 cohorts. (D-F) Survival analysis, receiver operating characteristic curve analysis, and PCA for the TCGA-BRCA cohort. (G-I) Equivalent analyses for the Vijver2002 cohort. TCGA, The Cancer Genome Atlas; BRCA, breast invasive carcinoma; UFAG, unsaturated fatty acids-related genes; PCA, principal component analysis; AUC, area under the curve; PC, principal component.

between these subtypes (*Figure 1E*).

Construction and evaluation of a UFAGs-derived risk signature

Lasso Cox regression yielded a risk signature comprised of 3 UFAGs (*Figure 2A*): risk score = –0.25169353 * *ACAA1* – 0.09111418 * *ACOT2* – 0.07883266 * *ELOVL2*. Stratification of the TCGA-BRCA and Vijver2002 cohorts into high- and low-risk groups by the median risk score is shown in *Figure 2B,2C*. High-risk patients in the TCGA-BRCA cohort had worse outcomes compared to low-risk patients (*Figure 2D*), with the risk score achieving AUC values of 0.584, 0.659, and 0.624 for predicting 1-, 3-, and 5-year overall survival (OS), respectively (*Figure 2E*). PCA depicted a clear distinction between risk groups (*Figure 2F*). Similar trends were observed in the Vijver2002 cohort, with high-risk patients having poorer survival (*Figure 2G*) and the risk score showing AUCs of 0.702, 0.62, and 0.62 for 1-, 3-, and 5-year OS prediction (*Figure 2H*), respectively. PCA confirmed distinct boundaries between risk groups (*Figure 2I*).

Clinical and pathological correlates of the UFAGs-related risk signature

Consistent downregulation of UFAGs related to the

risk signature in the high-risk group was noted, along with correlations to clinical characteristics (*Figure 3A*). Comparisons of risk scores across different clinical subgroups revealed that younger patients (<60 years) had higher risk scores compared to older patients (≥60 years), N3 stage patients had higher risk scores compared to N1 stage patients, patients with negative ER had higher risk scores compared to those with positive ER, patients with negative progesterone receptor (PR) had higher risk scores compared to those with positive PR, and patients with positive HER2 had higher risk scores compared to those with negative HER2. Additionally, patients with infiltrating ductal carcinoma (IDC) had higher risk scores compared to those with infiltrating lobular carcinoma (ILC). Furthermore, the Luminal A subtype had the lowest risk scores among all subtypes, while the Basal subtype had the highest risk scores (*Figure 3B*).

Association of the UFAGs-related risk signature with somatic mutations

The tumor mutation burden (TMB) was significantly lower in the low-risk group compared to the high-risk group (*Figure 4A*). Survival analysis illustrated differential outcomes between risk and TMB groups (*Figure 4B*), and a positive correlation was found between risk score and TMB (*Figure 4C*). The top 10 most frequently mutated genes in high- and low-risk groups are depicted in *Figure 4D,4E*.

Relationship of the UFAGs-related risk signature with the immune landscape

CIBERSORT analysis of TCGA-BRCA samples showed significant differences in immune infiltration patterns between risk groups, with low-risk patients exhibiting higher levels of B cells, mast cells, plasma cells, but lower M0 and M1 macrophages (*Figure 5A*). Low-risk patients also had elevated immune scores, ESTIMATE scores, and tumor purity (*Figure 5B-5E*), indicating an association between the UFAGs-related risk signature and the tumor immune microenvironment.

UFAGs-related risk signature correlated with chemotherapy sensitivity

Drug sensitivity analysis demonstrated that the low-risk group was more sensitive to 14 drugs including axitinib, bexarotene, and bicalutamide, while showing lower sensitivity to 21 drugs like bosutinib, camptothecin, and cisplatin (*Figure 6*). Significant correlations between UFAGs expression and drug sensitivity suggest a link between UFAs metabolism and therapeutic responsiveness.

Gene expression profiling in relation to the UFAGs-related risk signature

Differential expression analysis between risk groups led to KEGG and GO term enrichment analysis. Low-risk patients displayed enhanced activation of axoneme, cilium assembly, and cilium organization GO terms, while immune-related terms such as immunoglobulin complex, T cell receptor complex, antigen binding, and immunoglobulin production were suppressed (*Figure 7A*). Metabolic pathways including arachidonic acid (AA) metabolism and drug metabolism were upregulated, whereas cytokine signaling, natural killer (NK) cell activity, cell cycle, and interleukin (IL)-17 signaling pathways were downregulated in low-risk patients (*Figure 7B*).

UFAGs-related risk signature correlated with immunotherapy response

To evaluate the relationship between the UFAGs-related risk signature and the response to immunotherapy, we analyzed a cohort of BC patients undergoing anti-programmed cell death-ligand 1 (PD-L1) immunotherapy. Our results showed that compared to NR, CR had significantly lower expression levels of *ELOVL2* and *ACOT2*, while the expression of *ACAA1* remained unchanged (*Figure 8A*). The AUC values for predicting NR risk using *ACOT2*, *ELOVL2*, *ACAA1*, and the riskscore were 0.625, 0.703, 0.504, and 0.668, respectively (*Figure 8B-8E*). The proportion of CR patients was higher in the high-risk group compared to the low-risk group (*Figure 8F*), and the riskscore in the CR group were significantly higher than those in the NR group (*Figure 8G*). These findings are consistent with the TIDE analysis, which showed that the risk scores of true responders were significantly higher than those of false responders (*Figure 8H*). These results suggest that UFAGs are associated with the response to immunotherapy, and a higher UFAGs-related risk score correlates with better immunotherapy outcomes.

Nomogram incorporating the UFAGs-related risk signature

Univariate and multivariate Cox regression analyses

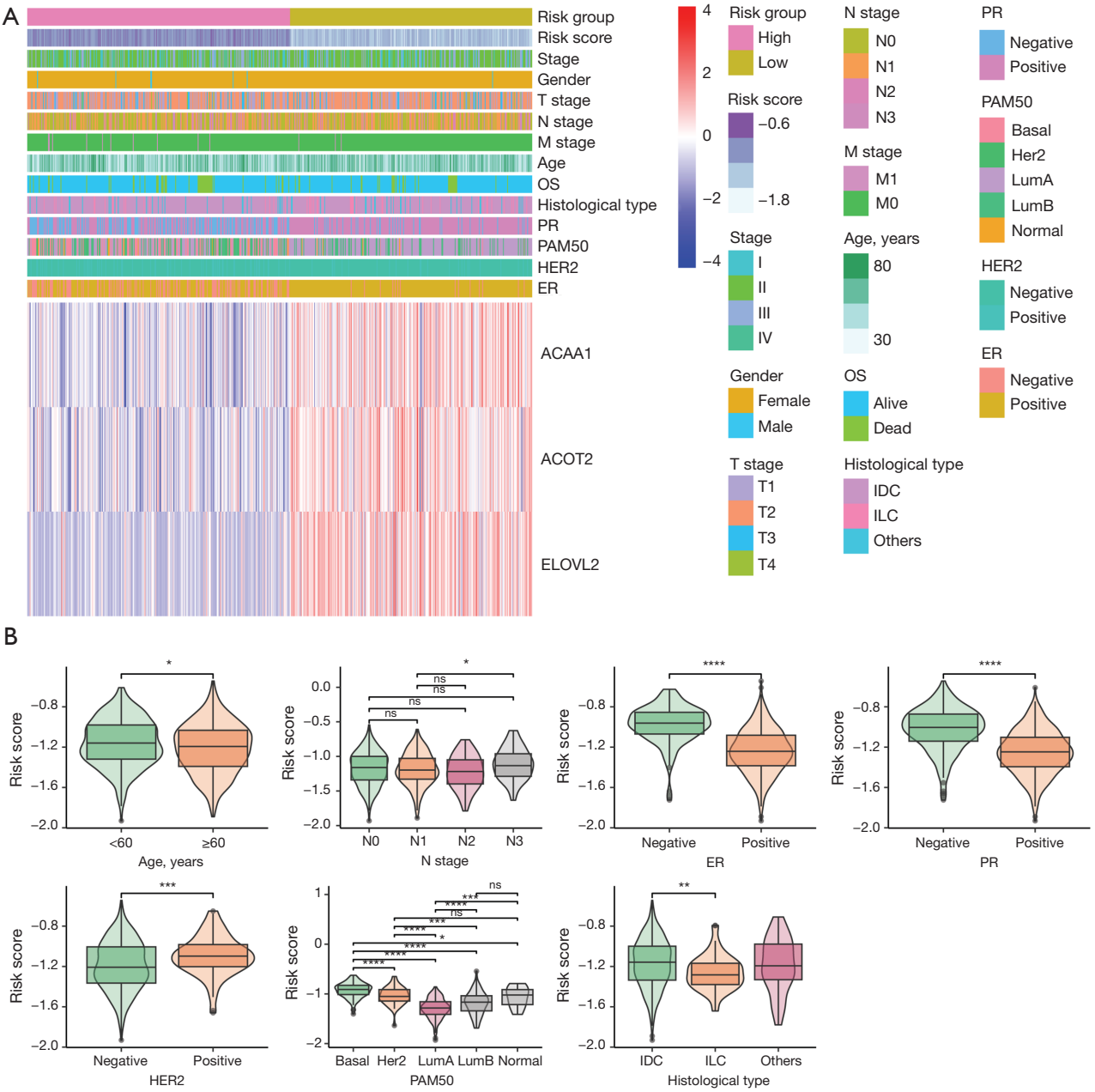

Figure 3 Association of risk signature with clinical-pathological features. (A) Heatmap of expression for risk signature-related UFAGs annotated with clinical-pathological information. (B) Comparative analysis of risk scores across different clinical-pathological subgroups. ns, not significant; *, P<0.05; **, P<0.01; ***, P<0.001; ****, P<0.0001. UFAG, unsaturated fatty acids-related genes; OS, overall survival; PR, progesterone receptor; HER2, human epidermal growth factor 2; ER, estrogen receptor; ACAA1, acetyl-CoA acyltransferase 1; ACOT2, acyl-CoA thioesterase 2; ELOVL2, ELOVL fatty acid elongase 2; IDC, infiltrating ductal carcinoma; ILC, infiltrating lobular carcinoma.

identified the riskscore and age as independent prognostic factors for BC (*Figure 9A,9B*). A nomogram integrating the riskscore and age was developed for convenient estimation of 1-, 3-, and 5-year OS in BC patients (*Figure 9C*). Calibration curves confirmed the accuracy of nomogram predictions against observed survival (*Figure 9D*). Decision curve analysis highlighted the nomogram's superiority over individual factors in BC prognosis, displaying a higher

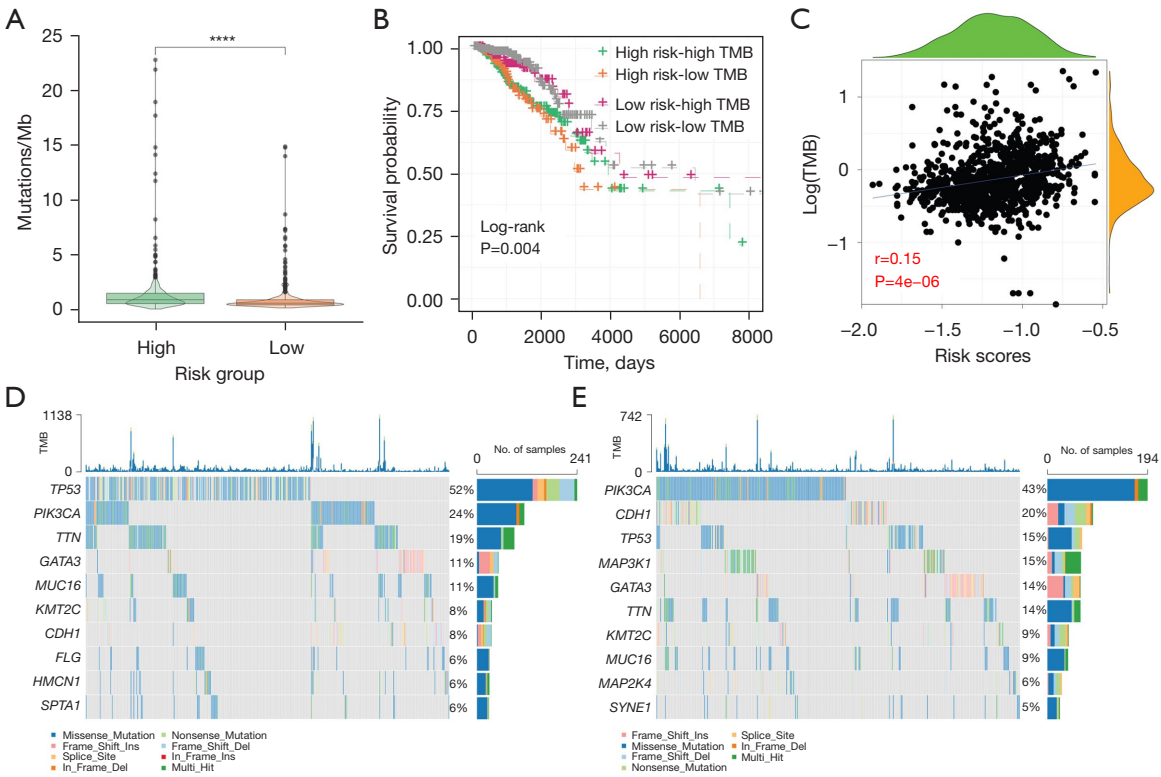

Figure 4 Relationship between risk signature and somatic mutations. (A) Comparison of TMB between high- and low-risk groups. ****, P<0.0001. (B) Survival analysis contrasting different risk and TMB groups. (C) Scatter plot depicting the correlation between risk score and TMB. (D,E) Top 10 most frequently mutated genes in high-risk and low-risk groups, respectively. TMB, tumor mutation burden.

standardized net benefit (*Figure 9E*). ROC analysis further supported the nomogram's outstanding performance with AUCs of 0.734, 0.675, and 0.657 for 1-, 3-, and 5-year OS prediction, respectively (*Figure 9F*), validating its excellence in BC prognosis assessment.

Discussion

UFAs, particularly ω-3 fatty acids like eicosapentaenoic acid (EPA) and docosahexaenoic acid (DHA), and ω-6 fatty acids such as AA, have been implicated in suppressing tumorigenesis, invasion, and metastasis, as reported in several studies (24,25). These lipids exert their effects through modulating inflammatory responses, inhibiting angiogenesis, inducing apoptosis in cancer cells, and enhancing chemosensitivity (26). Observations from multiple investigations link UFA intake to reduced incidence risks of various cancers, including breast, lung, and gastrointestinal cancers, potentially due to their immune-enhancing, anti-inflammatory, and antioxidative properties (27-29). Of note, ω-3 and ω-6 polyunsaturated fatty acids (PUFAs), through their immunomodulatory and inflammatory impacts, have emerged as pivotal regulators of carcinogenesis and progression, influencing both cancer cells and shaping the gut microbiota and immune landscape, as evidenced in colorectal and prostate cancer research (30,31). Therefore, elucidating the expression and prognostic significance of UFAGs in BC is of utmost importance for advancing our understanding of disease development and clinical intervention strategies.

In this study, leveraging gene expression and clinical data from TCGA, we initially identified five UFAGs significantly associated with BC prognosis. Through Lasso and Cox regression analyses, we established a prognostic model highlighting *ACAA1*, *ACOT2*, and *ELOVL2* as novel potential biomarkers. These three genes are integral to the synthesis and metabolism of UFAs, with lipid metabolic pathways playing a pivotal role in BC progression. *ACAA1* catalyzes the carboxylation of acetyl-CoA to malonyl-CoA, a key step in fatty acid synthesis, which is upregulated in BC,

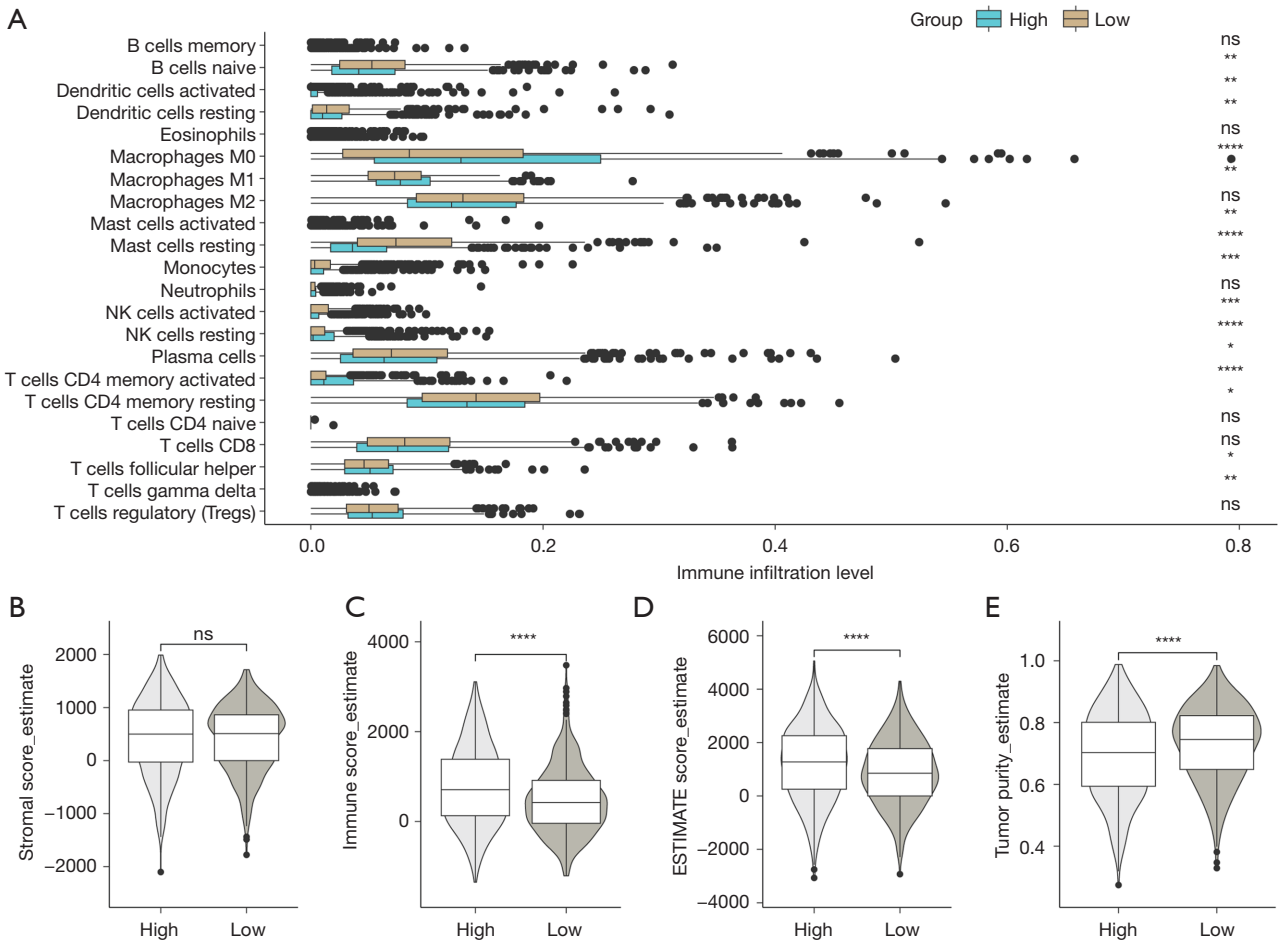

Figure 5 Association with the tumor immune microenvironment. (A) Comparison of immune cell infiltration between high- and low-risk groups. (B-E) Stromal score, immune score, ESTIMATE score, and tumor purity comparison between risk groups, respectively. ns, not significant; *, P<0.05; **, P<0.01; ***, P<0.001; ****, P<0.0001.

correlating with tumor proliferation and survival. Inhibition of *ACAA1* has been shown to suppress proliferation in triple-negative BC and enhance sensitivity to cyclin-dependent kinase (CDK) 4/6 inhibitors (32), underscoring its potential involvement in metabolic reprogramming for tumor growth. It is also recognized as a prognostic factor in various malignancies (33,34). *ACOT2*, a member of an enzyme family that hydrolyzes long-chain fatty acyl-CoAs, regulates cellular fatty acid levels and distribution, potentially affecting energy metabolism and signaling. Its elevation is linked to poor OS in acute myeloid leukemia and perturbed lipid metabolism, suggesting *ACOT2* as a promising therapeutic target (35). *ELOVL2* elongates fatty acids, contributing to the synthesis of long-chain fatty acids crucial for membrane fluidity, signaling, and inflammation control. Altered *ELOVL2* expression may disrupt the balance of these critical fatty acids. *ELOVL2* has been shown to inhibit prostate cancer proliferation, migration, and invasion via inositol polyphosphate-4-phosphatase type II B (*INPP4B*) regulation (36), and it is implicated in chemotherapy resistance and tumor progression in BC (37,38).

PD-L1 interaction with its receptor programmed cell death protein 1 (PD-1) on T cells negatively regulates T cell function, enabling immune evasion by cancer cells. Targeting PD-L1 is an attractive immunotherapeutic strategy in cancer, and ω-3 PUFAs like DHA can reduce PD-L1 expression in cancer cells both *in vitro* and *in vivo*. Our findings indicated that the riskscore derived from UFAGs were significantly higher in patients who respond to anti-PD-L1 therapy compared to NRs. Additionally, the expression levels of *ELOVL2* and *ACOT2* showed potential as biomarkers for predicting immune therapy response,

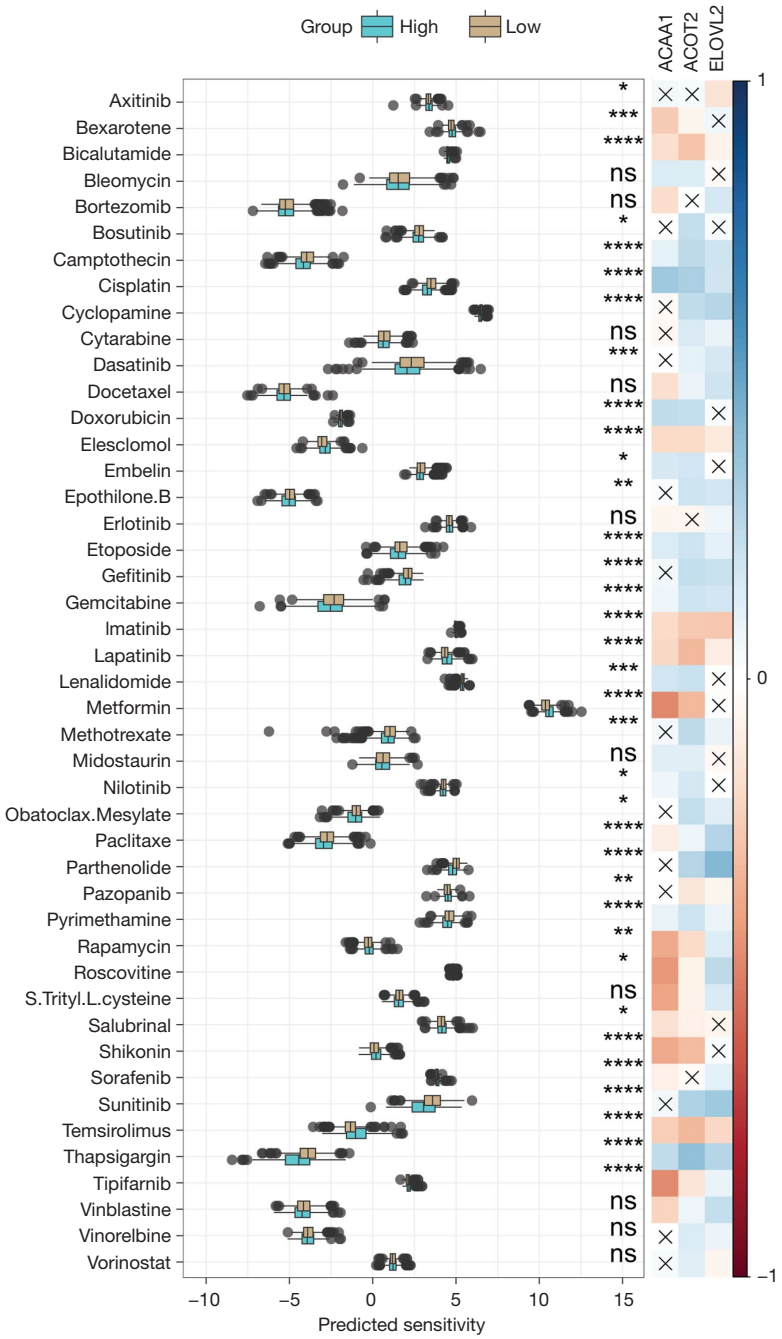

Figure 6 Differential drug sensitivity and heatmap showing correlations between risk signature-related UFAGs and drug sensitivity in high- and low-risk groups. ns, not significant; *, P<0.05; **, P<0.01; ***, P<0.001; ****, P<0.0001. UFAG, unsaturated fatty acids-related genes; ACAA1, acetyl-CoA acyltransferase 1; ACOT2, acyl-CoA thioesterase 2; ELOVL2, ELOVL fatty acid elongase 2.

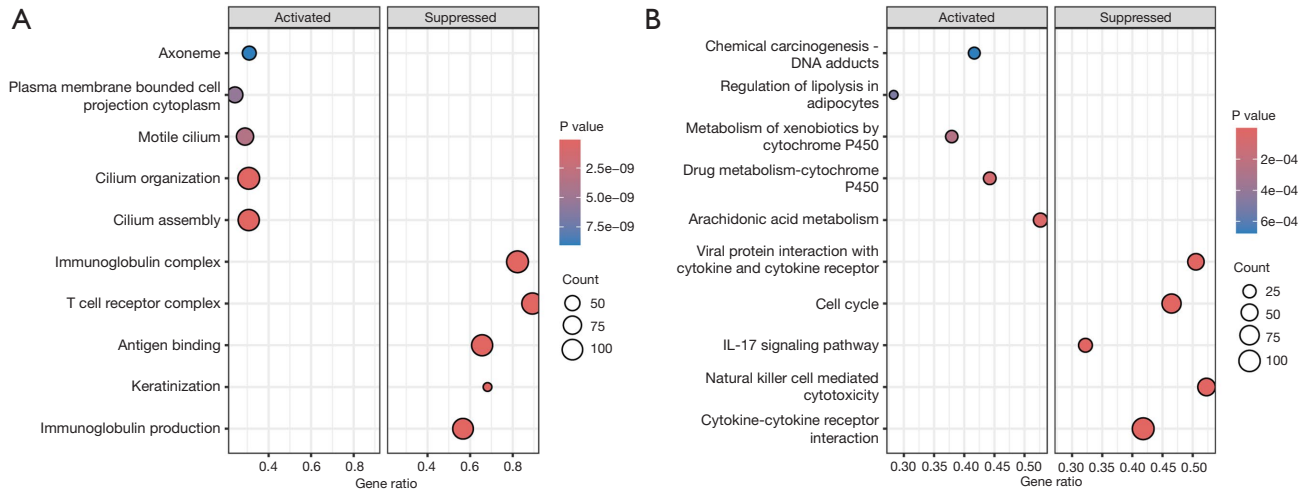

Figure 7 Association with gene expression patterns. (A) Gene Ontology term enrichment analysis. (B) Kyoto Encyclopedia of Genes and Genomes pathway enrichment analysis. IL, interleukin.

suggesting that targeting UFAGs may be a promising strategy to enhance the efficacy of immune therapy. Given that *ELOVL2* is a rate-limiting enzyme in DHA synthesis, the impact of *ELOVL2* on the response to immunotherapy may not be mediated through the accumulation of DHA. DHA promotes PD-L1 proteasomal degradation, reducing its expression and interaction with PD-1, thereby reversing PD-L1-mediated immune suppression and tumor growth inhibition (39). Monounsaturated fatty acids also decrease PD-L1 expression, implicating their role in immune response modulation. Animal models suggest potential synergistic therapy combining anti-PD-1 treatment with Ω-3 PUFA supplementation in esophageal squamous cell carcinoma (40). A recent study demonstrated that feeding DHA alone or in combination with alpha-linolenic acid reduced hepatic ELOVL2 activity (41), indicating that DHA may enhance immune therapy response by inhibiting *ELOVL2* activity. Therefore, the role and mechanisms of UFAGs, particularly in the context of BC immune therapy response, warrant further investigation.

Chemotherapy resistance poses a substantial challenge to successful cancer treatment outcomes, and dysregulation of fatty acid metabolism genes may contribute to this resistance. DHA and EPA, two n-3 PUFAs, have garnered attention for their potential to alter membrane lipid composition and modulate the expression of cancer-related genes such as B-cell lymphoma-2 (Bcl-2), phosphatidylinositol 3-kinase (PI3K), nuclear factor kappa B subunit 1 (NK-κB), and phosphorylated AKT serine/threonine kinase 1, potentially mitigating cancer risk (42-44). They also show promise in enhancing chemotherapeutic efficacy, particularly in resistant cells (44,45). The UFAGs-related risk signature developed herein exhibits a significant association with drug sensitivity, possibly mediated through UFA biosynthesis. *ACAA1* interacts with CDK4, and its inhibition blocks RB1 phosphorylation, leading to G1-S cell cycle arrest, with reduced ACAA1 protein levels augmenting abemaciclib's effectiveness (32). *ELOVL2* has been shown to partially restore tamoxifen sensitivity in MCF-7/TamR cells and xenograft models, regulating a set of genes, including *THEM4*, involved in AKT and ERα signaling pathways crucial for resistance (37).

Despite these findings, our study has limitations. Primarily, the retrospective nature of the cohort analysis used for risk signature and nomogram construction lacks prospective validation, limiting immediate clinical applicability. Additionally, functional analyses of risk signature genes and their mechanistic roles in BC development lack *in vitro* and *in vivo* experimental validations.

Conclusions

In summary, this study systematically investigated the expression, mutational status, and prognostic relevance of UFAGs in BC, leading to the construction of molecular subtypes and a risk profile based on prognosis-associated UFAGs. We elucidated the associations between the UFAGs-related risk profile and clinical-pathological characteristics, somatic features, gene expression patterns, tumor immune

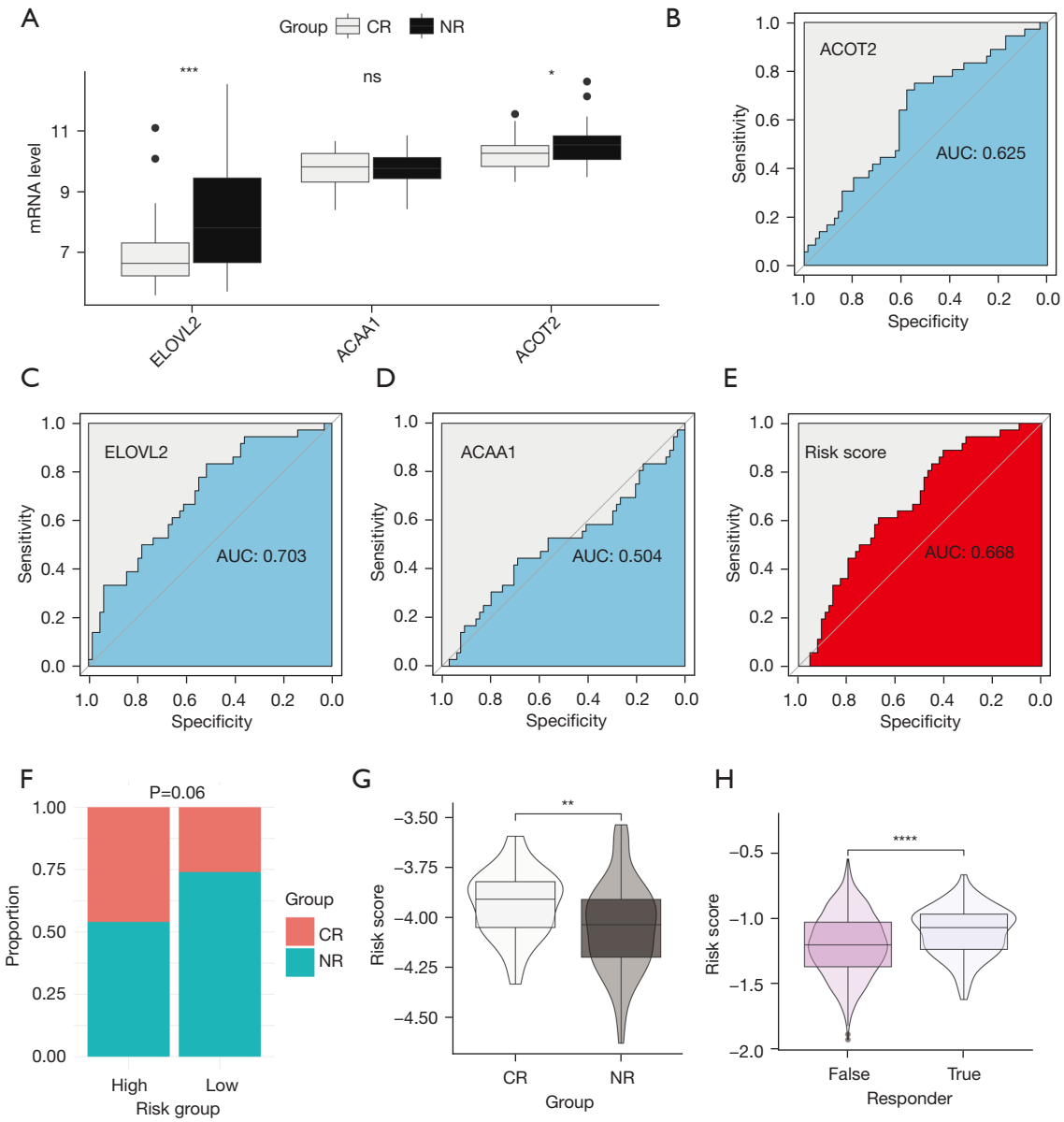

Figure 8 Relationship between UFAGs-derived risk signature and immune therapy response. (A) Comparison of UFAGs expression between immune therapy responders and non-responders in the GSE173839 cohort. ROC curve analysis for predicting immune therapy response using (B) ACOT2, (C) ELOVL2, (D) ACAA1 and (E) risk score in the GSE173839 cohort. (F) Comparison of the proportion of immune therapy responders between the high- and low-risk groups in the GSE173839 cohort. (G) Comparison of risk score between responders and non-responders in the GSE173839 cohort. (H) Comparison of risk score between true responders and false responders as assessed by TIDE. ns, not significant; *, P<0.05; **, P<0.01; ***, P<0.001; ****, P<0.0001. UFAG, unsaturated fatty acids-related genes; ACOT2, acyl-CoA thioesterase 2; ELOVL2, ELOVL fatty acid elongase 2; ACAA1, acetyl-CoA acyltransferase 1; TIDE, Tumor Immune Dysfunction and Exclusion; CR, complete responder; NR, non-responder; AUC, area under the curve.

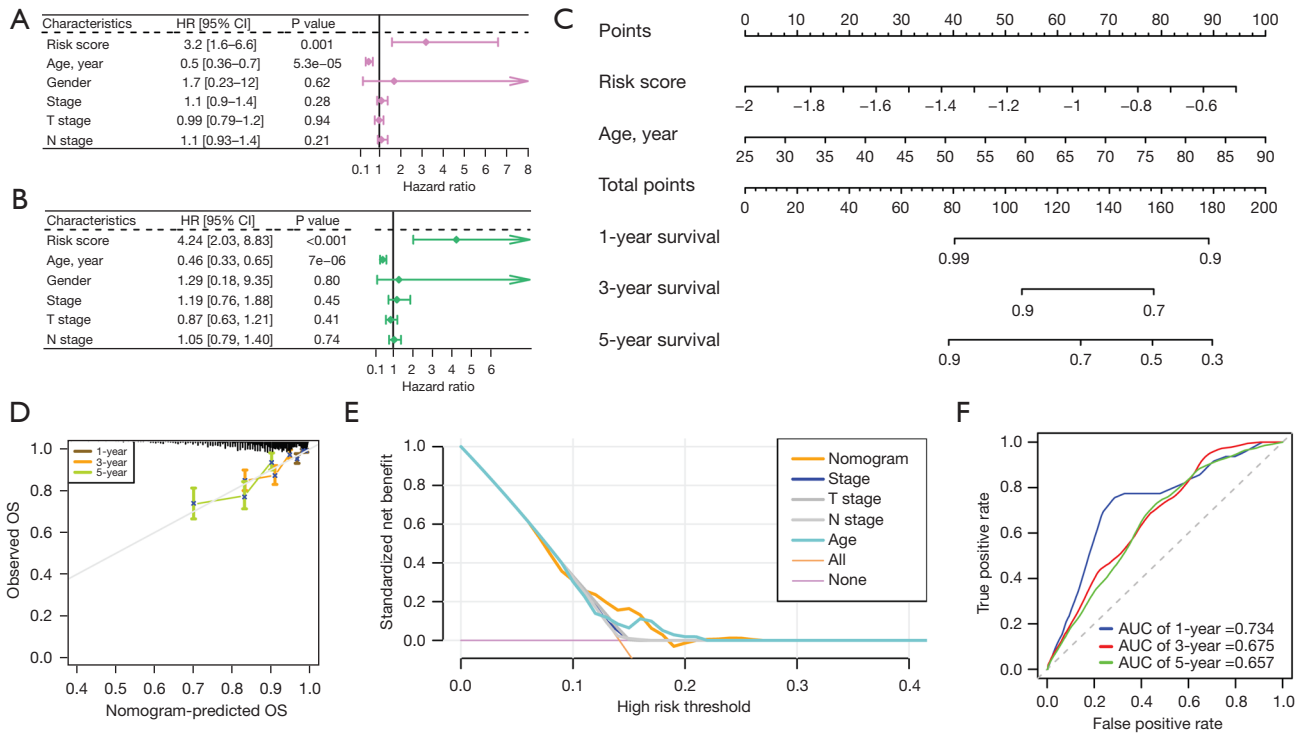

Figure 9 Nomogram construction and evaluation based on UFAGs-related risk signature. (A,B) Univariate and multivariate Cox regression analyses. (C) Nomogram integrating risk score and age for predicting 1-, 3-, and 5-year OS in breast cancer. (D) Calibration curve, (E) decision curve, and (F) ROC analysis for nomogram validation. UFAG, unsaturated fatty acids-related genes; ROC, receiver operating characteristic; HR, hazard ratio; OS, overall survival; AUC, area under the curve; CI, confidence interval.

microenvironment, drug sensitivity, and responsiveness to immunotherapy in BC patients. Ultimately, a nomogram was devised for prognostic assessment in BC by integrating the risk score with patient age. Nevertheless, the validity of the UFAGs-derived risk signature and nomogram necessitates further corroboration through prospective clinical investigations, while the underlying biological roles of UFAGs in BC pathophysiology require more extensive exploration.

Acknowledgments

None.

Footnote

Reporting Checklist: The authors have completed the TRIPOD reporting checklist. Available at https://tcr.amegroups.com/article/view/10.21037/tcr-24-1668/rc

Peer Review File: Available at https://tcr.amegroups.com/article/view/10.21037/tcr-24-1668/prf

Funding: This study was supported by Zhejiang Provincial Natural Science Foundation of China (No. LQ21H290004).

Conflicts of Interest: All authors have completed the ICMJE uniform disclosure form (available at https://tcr.amegroups.com/article/view/10.21037/tcr-24-1668/coif). The authors have no conflicts of interest to declare.

Ethical Statement: The authors are accountable for all aspects of the work in ensuring that questions related to the accuracy or integrity of any part of the work are appropriately investigated and resolved. The study was conducted in accordance with the Declaration of Helsinki (as revised in 2013).

References

1. Sung H, Ferlay J, Siegel RL, et al. Global Cancer Statistics 2020: GLOBOCAN Estimates of Incidence and Mortality Worldwide for 36 Cancers in 185 Countries. CA Cancer J Clin 2021;71:209-49.
2. Liang Y, Zhang H, Song X, et al. Metastatic heterogeneity of breast cancer: Molecular mechanism and potential therapeutic targets. Semin Cancer Biol 2020;60:14-27.
3. Bryan S, Witzel I, Borgmann K, et al. Molecular Mechanisms Associated with Brain Metastases in HER2-Positive and Triple Negative Breast Cancers. Cancers (Basel) 2021;13:4137.
4. Pegram M, Jackisch C, Johnston SRD. Estrogen/HER2 receptor crosstalk in breast cancer: combination therapies to improve outcomes for patients with hormone receptor-positive/HER2-positive breast cancer. NPJ Breast Cancer 2023;9:45.
5. Pu M, Messer K, Davies SR, et al. Research-based PAM50 signature and long-term breast cancer survival. Breast Cancer Res Treat 2020;179:197-206.
6. Barzaman K, Karami J, Zarei Z, et al. Breast cancer: Biology, biomarkers, and treatments. Int Immunopharmacol 2020;84:106535.
7. Vriens K, Christen S, Parik S, et al. Evidence for an alternative fatty acid desaturation pathway increasing cancer plasticity. Nature 2019;566:403-6.
8. Taborda Ribas H, Sogayar MC, Dolga AM, et al. Lipid profile in breast cancer: From signaling pathways to treatment strategies. Biochimie 2024;219:118-29.
9. Chen Y, Zhou Y, Ren R, et al. Harnessing lipid metabolism modulation for improved immunotherapy outcomes in lung adenocarcinoma. J Immunother Cancer 2024;12:e008811.
10. Melana JP, Mignolli F, Stoyanoff T, et al. The Hypoxic Microenvironment Induces Stearoyl-CoA Desaturase-1 Overexpression and Lipidomic Profile Changes in Clear Cell Renal Cell Carcinoma. Cancers (Basel) 2021;13:2962.
11. Nakagawa H, Hayata Y, Kawamura S, et al. Lipid Metabolic Reprogramming in Hepatocellular Carcinoma. Cancers (Basel) 2018;10:447.
12. Coradini D. Impact of De Novo Cholesterol Biosynthesis on the Initiation and Progression of Breast Cancer. Biomolecules 2024;14:64.
13. Tabe Y, Konopleva M, Andreeff M. Fatty Acid Metabolism, Bone Marrow Adipocytes, and AML. Front Oncol 2020;10:155.
14. Welty FK, Daher R, Garelnabi M. Fish and Omega-3 Fatty Acids: Sex and Racial Differences in Cardiovascular Outcomes and Cognitive Function. Arterioscler Thromb Vasc Biol 2024;44:89-107.
15. Deng W, Yi Z, Yin E, et al. Effect of omega-3 polyunsaturated fatty acids supplementation for patients with osteoarthritis: a meta-analysis. J Orthop Surg Res 2023;18:381.
16. Wibowo AA, Willyanto NA. The efficacy of omega-3 fatty acids (O3FAs) as a complementary in colorectal cancer patients: A systematic review and meta-analysis. Clin Nutr ESPEN 2024;61:322-32.
17. Mei J, Qian M, Hou Y, et al. Association of saturated fatty acids with cancer risk: a systematic review and meta-analysis. Lipids Health Dis 2024;23:32.
18. Gelsomino G, Corsetto PA, Campia I, et al. Omega 3 fatty acids chemosensitize multidrug resistant colon cancer cells by down-regulating cholesterol synthesis and altering detergent resistant membranes composition. Mol Cancer 2013;12:137.
19. Silva JA, Colquhoun A. Effect of Polyunsaturated Fatty Acids on Temozolomide Drug-Sensitive and Drug-Resistant Glioblastoma Cells. Biomedicines 2023;11:779.
20. Wilkerson MD, Hayes DN. ConsensusClusterPlus: a class discovery tool with confidence assessments and item tracking. Bioinformatics 2010;26:1572-3.
21. Wu T, Hu E, Xu S, et al. clusterProfiler 4.0: A universal enrichment tool for interpreting omics data. Innovation (Camb) 2021;2:100141.
22. Zeng D, Ye Z, Shen R, et al. IOBR: Multi-Omics Immuno-Oncology Biological Research to Decode Tumor Microenvironment and Signatures. Front Immunol 2021;12:687975.
23. Geeleher P, Cox N, Huang RS. pRRophetic: an R package for prediction of clinical chemotherapeutic response from tumor gene expression levels. PLoS One 2014;9:e107468.
24. Giordano C, Plastina P, Barone I, et al. n-3 Polyunsaturated Fatty Acid Amides: New Avenues in the Prevention and Treatment of Breast Cancer. Int J Mol Sci 2020;21:2279.
25. Kiyasu Y, Zuo X, Liu Y, et al. EPA, DHA, and resolvin effects on cancer risk: The underexplored mechanisms. Prostaglandins Other Lipid Mediat 2024;174:106854.
26. Murray M. Omega-3 polyunsaturated fatty acid derived lipid mediators: a comprehensive update on their application in anti-cancer drug discovery. Expert Opin Drug Discov 2024;19:617-29.

27. Moon YA. Emerging roles of polyunsaturated fatty acid synthesis pathway in colorectal cancer. Anim Cells Syst (Seoul) 2023;27:61-71.
28. Sheeter DA, Garza S, Park HG, et al. Unsaturated Fatty Acid Synthesis Is Associated with Worse Survival and Is Differentially Regulated by MYCN and Tumor Suppressor microRNAs in Neuroblastoma. Cancers (Basel) 2024;16:1590.
29. Thanikachalam K, Khan G. Colorectal Cancer and Nutrition. Nutrients 2019;11:164.
30. Lachance G, Robitaille K, Laaraj J, et al. The gut microbiome-prostate cancer crosstalk is modulated by dietary polyunsaturated long-chain fatty acids. Nat Commun 2024;15:3431.
31. Tojjari A, Choucair K, Sadeghipour A, et al. Anti-Inflammatory and Immune Properties of Polyunsaturated Fatty Acids (PUFAs) and Their Impact on Colorectal Cancer (CRC) Prevention and Treatment. Cancers (Basel) 2023;15:4294.
32. Peng WT, Jin X, Xu XE, et al. Inhibition of ACAA1 Restrains Proliferation and Potentiates the Response to CDK4/6 Inhibitors in Triple-Negative Breast Cancer. Cancer Res 2023;83:1711-24.
33. Feng H, Shen W. ACAA1 Is a Predictive Factor of Survival and Is Correlated With T Cell Infiltration in Non-Small Cell Lung Cancer. Front Oncol 2020;10:564796.
34. Zhang X, Yang H, Zhang J, et al. HSD17B4, ACAA1, and PXMP4 in Peroxisome Pathway Are Down-Regulated and Have Clinical Significance in Non-small Cell Lung Cancer. Front Genet 2020;11:273.
35. Yin X, Lyu C, Li Z, et al. High Expression of ACOT2 Predicts Worse Overall Survival and Abnormal Lipid Metabolism: A Potential Target for Acute Myeloid Leukemia. J Healthc Eng 2022;2022:2669114.
36. Hu T, Zhang H, Du Y, et al. ELOVL2 restrains cell proliferation, migration, and invasion of prostate cancer via regulation of the tumor suppressor INPP4B. Cell Signal 2022;96:110373.
37. Jeong D, Ham J, Kim HW, et al. ELOVL2: a novel tumor suppressor attenuating tamoxifen resistance in breast cancer. Am J Cancer Res 2021;11:2568-89.
38. Kang YP, Yoon JH, Long NP, et al. Spheroid-Induced Epithelial-Mesenchymal Transition Provokes Global Alterations of Breast Cancer Lipidome: A Multi-Layered Omics Analysis. Front Oncol 2019;9:145.
39. Zhang H, Chen H, Yin S, et al. Docosahexaenoic acid reverses PD-L1-mediated immune suppression by accelerating its ubiquitin-proteasome degradation. J Nutr Biochem 2023;112:109186.
40. Xiao X, Luo S, Huang J, et al. Synergistic effects of Ω-3 polyunsaturated fatty acid supplementation and programmed cell death protein 1 blockade on tumor growth and immune modulation in a xenograft model of esophageal cancer. Clin Nutr ESPEN 2024;61:308-15.
41. Metherel AH, Valenzuela R, Klievik BJ, et al. Dietary docosahexaenoic acid (DHA) downregulates liver DHA synthesis by inhibiting eicosapentaenoic acid elongation. J Lipid Res 2024;65:100548.
42. Chauvin L, Goupille C, Blanc C, et al. Long chain n-3 polyunsaturated fatty acids increase the efficacy of docetaxel in mammary cancer cells by downregulating Akt and PKCε/δ-induced ERK pathways. Biochim Biophys Acta 2016;1861:380-90.
43. Shao ZC, Zhu BH, Huang AF, et al. Docosahexaenoic Acid Reverses Epithelial-Mesenchymal Transition and Drug Resistance by Impairing the PI3K/AKT/ Nrf2/ GPX4 Signalling Pathway in Docetaxel-Resistant PC3 Prostate Cancer Cells. Folia Biol (Praha) 2022;68:59-71.
44. Zhang Y, Shen G, Meng T, et al. Eicosapentaenoic acid enhances the sensitivity of osteosarcoma to cisplatin by inducing ferroptosis through the DNA-PKcs/AKT/NRF2 pathway and reducing PD-L1 expression to attenuate immune evasion. Int Immunopharmacol 2023;125:111181.
45. Gurav P, Garad S, Nirmala KR. n-3 PUFAs Show Promise as Adjuvants in Chemotherapy, Enhancing their Efficacy while Safeguarding Hematopoiesis and Promoting Bone Generation. Curr Top Med Chem 2024;24:45-59.

Cite this article as: Meng H, Zhang S, Ling M, Hu Y, Xie X. Construction of a prognostic signature for breast cancer based on genes involved in unsaturated fatty acid biosynthesis. Transl Cancer Res 2025;14(2):1190-1204. doi: 10.21037/tcr-24-1668